

Hard core-soft shell particles near repulsive interfaces: interplay between adsorption, aggregation and diffusion

Murilo S. Marques^{†,‡} and José Rafael Bordin^{*,¶}

[†]*Centro das Ciências Exatas e das Tecnologias, Campus Reitor Edgard Santos, Universidade Federal do Oeste da Bahia, Rua Bertioga, 892, CEP 47810-059, Barreiras, Bahia, Brazil*

[‡]*Instituto de Física, Universidade Federal do Rio Grande do Sul, Caixa Postal 15051, CEP 91501-970, Porto Alegre, Rio Grande do Sul, Brazil*

[¶]*Departamento de Física, Instituto de Física e Matemática, Universidade Federal de Pelotas. Caixa Postal 354, 96001-970, Pelotas, Brazil.*

E-mail: jrbordin@ufpel.edu.br

Abstract

The behavior of colloidal particles with a hard core and a soft shell has attracted the attention for researchers in the physical-chemistry interface not only due the large number of applications, but due the unique properties of these systems in bulk and at interfaces. The adsorption at the boundary of two phases can provide information about the molecular arrangement. In this way, we perform Langevin Dynamics simulations of polymer-grafted nanoparticles. We employed a recently obtained core-softened potential to analyze the relation between adsorption, structure and dynamic properties of the nanoparticles near a solid repulsive surface. Two cases were considered: flat or structured walls. At low temperatures, a maxima is observed in the adsorption. It is

related to a fluid to clusters transition and with a minima in the contact layer diffusion - and is explained by the competition between the scales in the core-softened interaction. Due the long range repulsion, the particles stay at the distance correspondent to this length scale at low densities, and overcome the repulsive barrier as the packing increases, However, increasing the temperature, the gain in kinetic energy allows the colloids to overcome the long range repulsion barrier even at low densities. As consequence, there is no competition and no maxima was observed in the adsorption.

Introduction

A multitude of natural process take place at the boundary between two phases while others are started at that interface. This is the case of adsorption¹ - a universal phenomenon in colloidal and surface science² whose properties have been studied for a long time.³⁻⁵ Basically, it's a surface effect which causes affluence (change in concentration) of atoms, molecules or ions at two-phase interfaces⁶ drastically modifying its properties compared to bulk.⁷ For spherical colloids and nanoparticles, macromolecules that often show competitive interactions,^{8,9} the adsorption and binding at interfaces associated with the various probabilities of aggregation are fundamental for applications in biomedical, environmental, food, and materials engineering.¹⁰⁻¹³ In this context, the computational simulation of colloids at interfaces have evolved enormously and nowadays the structure, dynamics, thermodynamics, phase transitions, and reactivity of colloids in confined environments and interfacial geometries have been widely studied,¹³⁻¹⁶ mainly through attractive and repulsive competing interactions.¹⁷ Such interrelation had as their starting point the famous DVLO theory for charged colloids at 1940's¹⁸ and the seminal work of Asakura and Oosawa (AO) at 1950's:^{19,20} these two approaches provide a framework by which attraction and repulsion between colloids may be manipulated.²¹

Today the current stage of modeling has brought to us a variety of potentials that have being used to portray the competitive interactions between spherical colloids. The competi-

tions, usually between a Short range Attraction and a Long range Repulsion – the so-called SALR colloids, arise once distinct conformations compete to rule the suspension behavior.^{22–24} The short range attraction is caused by van der Waals forces or solvent effects,²⁵ while the long range repulsion can be generated by many factors. For instance, it can be caused by electrostatic repulsion in charged colloids and molecules,^{26,27} or by soft shells as in the case of spherical colloids obtained by PEG aggregates^{28–30} or even by a polymeric brush, as metallic NP^{31–35} decorated with polymers and star polymers.³⁶

From experimental^{28,29} and computational^{31,32} works, it is well known that the SALR NP and colloids effective interaction can be depicted by core-softened potentials. In this way, many works have been devoted to study the behavior of competitive colloidal systems in bulk solutions.^{37–42} There are a plenty of works exploring the behavior of confined SALR systems in recent times: Almaraz et al have inspected the template-assisted pattern formation in monolayers of particles by Monte Carlo simulations in a lattice gas generic model;^{25,43} Litniewski and Ciach have analyzed the general features of adsorption phenomena in dilute systems with particles self-assembling into small clusters;^{44,45} more recently, Panagiotopoulos et al have scrutinized properties of lamellar structures formed by an SALR fluid in equilibrium and non-equilibrium conditions by machine learning;⁴⁶ Bilnadau et al investigated the cluster formation effect on adsorption phenomena they have laid down deviation in the shape of the adsorption isotherm in comparison with simple fluids.⁴⁷ Though, according to the authors’ knowledge, no relationship between aggregation, adsorption and dynamic management was listed in these SALR colloids at interfaces. In this work, we have looked over the behavior of a SALR system confined by two types of plates: rough and flat, and we’ve explored the distinctness of adsorption isotherms, lateral structuring (by means of the lateral radial distribution function) and the dynamic behavior of the system in order to answer the question: how the surface smoothness influence the adsorption in systems shaped by competitive interactions?

The answer to this inquiry is organized as follows. In Sec. II, we provide details of model

and simulation details, while results and theoretical approach are presented and discussed in Sec. III. Conclusions follow in Sec. IV.

The Model and Simulation Details

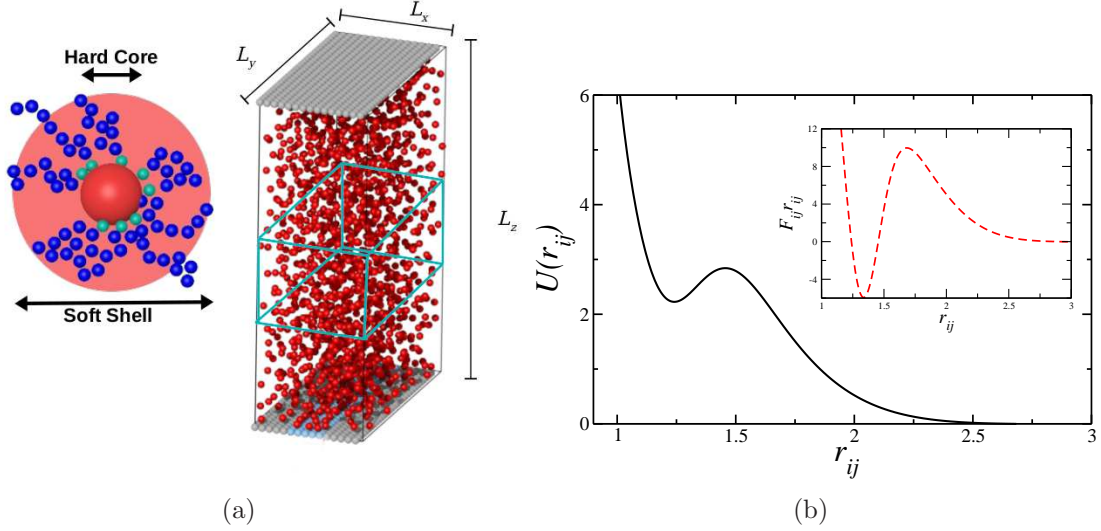


Figure 1: (a) Schematic depiction of the polymer-grafted NP and simulations box. In the NP, the blue monomers stand for the polymers, the green is the monomer connected to the hard-core red bead. The simulation box with size $L_x \times L_y \times L_z$ in the x , y and z directions has two walls in the z -extremes. The turquoise lines represents the density control volume region. (b) Effective potential $U(r_{ij})$ employed to model the colloids as obtained in our recent work.³¹ The inset is the product of the pair force $F_{ij} = -dU(r_{ij})/dr_{ij}$ and the distance r_{ij} as function of the distance.

The fluid consists of spherical nanoparticles (NP) with a hard core and a soft corona, as schematically depicted in the figure 1(a). The effective core-softened interaction potential, obtained in a recent work by Marques and co-authors,³¹ is composed by a short-range attractive Lennard Jones potential and three Gaussian terms, each one centered in c_j , with depth h_j and width w_j :

$$U(r_{ij}) = 4\epsilon \left[\left(\frac{\sigma}{r_{ij}} \right)^{12} - \left(\frac{\sigma}{r_{ij}} \right)^6 \right] + \sum_{j=1}^3 h_j \exp \left[- \left(\frac{r_{ij} - c_j}{w_j} \right)^2 \right], \quad (1)$$

Here, $r_{ij} = |\vec{r}_i - \vec{r}_j|$ is the distance between two particles i and j . The Gaussian parameters

are given in table 1. With these parameters, the interaction potential has a shoulder-like shape and two characteristic interaction length scales,^{48–51} as shown in the figure 1(b). A closer length scale, located near 1.2σ , that stands for the hard-core, and a further second scale $r_{ij} \approx 2.2\sigma$ from the soft-corona. Between them there is a entropic barrier - the scales and the barrier are clear in the inset of the figure 1(b).

Table 1: Interacting potential parameters in reduced units.

Parameter	Value
h_1	3.50803
c_1	1.05317
w_1	0.0887196
h_2	3.2397
c_2	1.37689
w_2	0.468399
h_3	-3.8685
c_3	1.1684
w_3	0.2400

Langevin Dynamics simulations were performed with a time step of $\delta t = 0.01$ and $\gamma = 1.0$ using the ESPResSo package.^{52,53} The simulation box has dimensions $L_x = 15\sigma$, $L_y = 30\sigma$ and $L_z = 45\sigma$. The adsorption surfaces are confining plates placed in the limits of the z -direction. $V_F = [L_x \times L_y \times (L_z - 2.0)]$ is the available volume for the particles considering the excluded volume from the wall particles. Periodic boundary conditions were applied in the x and y -directions.

The confining plates can be flat or rough. In the rough case they are modeled as spherical particles with diameter σ distributed in a square lattice and fixed in space. The interaction between the wall and fluid particles is given by the purely repulsive Weeks-Chandler-Andersen (WCA) potential. The WCA interaction is a LJ interaction – first therm in Equation 1 – cut at $r_{ij} = 2^{\frac{1}{6}}\sigma$ and shifted by ϵ . In the flat case the wall was considered as a plane that repels the fluid by the projection of the WCA potential in the z -direction - interacting as a structureless flat surface.

Simulations were performed with different bulk number density, ranging from $\rho_0 =$

$N_0/V_F = 0.025\sigma^3$ to $\rho_0 = 0.200\sigma^3$ and temperatures from $T = 0.1\epsilon/k_B$ to $T = 0.90\epsilon/k_B$. The initial number of particles in the system, obtained from $N_0 = \rho_0 V_F$, were initially randomly distributed in the simulation box. However, considering that particles will adsorb and get structured near to the wall, we create a Control Volume (CV) at the center of the simulation box to control the bulk density ρ_0 , as depicted in the figure 1(a). The control volume has dimensions $L_x \times L_y \times L_z/3$. Unlike previous works, where a Grand Canonical Monte Carlo simulation was used to keep the chemical potential fixed in a CV,⁵⁴⁻⁵⁶ here we adopted a simpler and faster approach: we control the density in the CV at every 500 time steps during the thermalization steps. If it deviated more than 2% from the initial value ρ_0 we insert/remove particles to restore the desired density. We check for overlaps and new particles are inserted with a initial velocity obtained from a Gaussian distribution at the proper thermal energy. We observe that after 5×10^5 thermalization steps the density in the CV do not deviates more than 2% from the mean value and, therefore, no more insertion/deletion moves are performed. The thermalization steps are followed by 5×10^5 steps to equilibrate the system. Finally, we run 2×10^6 steps for the results production stage. To ensure that the system was thermalized, the pressure, kinetic and potential energy were analyzed as function of time. The velocity-verlet algorithm was employed to integrate the equations of motion. 5 independent simulations (distinct initial random positions and velocities) were performed and here we present the average of this 5 results – the errors bars are smaller than the points in the results shown in Section .

The Gibbs adsorption isotherms were evaluated using

$$\Gamma(\rho_0) = \int_0^\infty [\rho(z) - \rho_0] dz, \quad (2)$$

where $\rho(z)$ is the density profile along the z -direction and ρ_0 the density in the CV. The lateral dynamics in the non-confined plane was analyzed by the relation between the lateral

mean square displacement (LMSD) and time, namely

$$\langle [r(t) - r(t_0)]^2 \rangle = \langle \Delta r^2(t) \rangle, \quad (3)$$

where $r(t_0) = (x^2(t_0) + y^2(t_0))^{1/2}$ and $r(t) = (x^2(t) + y^2(t))^{1/2}$ denote the coordinate of the particle at a time t_0 and at a later time t , respectively. The LMSD is related to the diffusion coefficient D by⁵⁷

$$D = \lim_{t \rightarrow \infty} \frac{\langle \Delta r^2(t) \rangle}{4t}. \quad (4)$$

The structure of the fluid was analyzed using the lateral radial distribution function (RDF) $g_{||}(r_{ij})$,⁵⁸

$$g_{||}(r_{ij}) \equiv \frac{1}{\rho^2 V} \sum_{i \neq j} \delta(r - r_{ij}) [\theta(|z_i - z_j|) - \theta(|z_i - z_j| - \delta z)] \quad (5)$$

where the Heaviside function $\theta(x)$ restricts the sum of particles pairs in a slab of thickness $\delta z = 1.5\sigma$.

The clustering was analyzed based in the inter particle bonding.^{59–61} Two particles in a layer belong to the same cluster if the distance between two of them is shorter than a cutoff 1.3 - a value slightly bigger than the first length scale. n_c is the number of particles in each cluster, and $P(n_c)$ the probability to find a cluster with size n_c .

In this work all the quantities are computed and presented in the standard Lennard Jones (LJ) reduced units,⁵⁷

$$r^* \equiv \frac{r}{\sigma}, \quad \rho^* \equiv \rho \sigma^3, \quad \text{and} \quad t^* \equiv t \left(\frac{\epsilon}{m \sigma^2} \right)^{1/2}, \quad (6)$$

for distance, density of particles and time, respectively, and

$$p^* \equiv \frac{p \sigma^3}{\epsilon} \quad \text{and} \quad T^* \equiv \frac{k_B T}{\epsilon} \quad (7)$$

for the pressure and temperature, respectively, where $\sigma = 1.4$ nm, $\epsilon_{core}/k_B = 10179$ K, with

k_B the Boltzmann constant, are the distance and energy parameters as previously works.^{31,32} m is the mass of a single NP. Since all physical quantities are defined in reduced LJ units, the * will be omitted, in order to simplify the discussion.

Results and discussion

To analyze the layering near the surfaces we have evaluated the density profile along the confining direction. In figure 2 we show the densities profiles $\rho(z)$ normalized by the bulk density ρ_0 . To analyze the properties of distinct fluid layers we have sliced the system in slabs with thickness $\delta z = 1.5$. Then, we select three slabs: the contact slab (I), that ranges from $z = 0.0$ to $z = 1.5$, one slab in the bulk region (III), from $z = 13.5$ to $z = 15.0$, and a intermediate slab (II) from $z = 6.0$ to $z = 7.5$, as indicated by the vertical dotted lines in the figure 2.

As expected, the layering is influenced by the temperature - and so adsorption isotherm with distinct behaviors. System at the smaller temperature have a layering that can span to the entire simulation box - as we can see for $T = 0.10$ and $\rho = 0.100$ for both surfaces. For higher temperature there is only the creation of a contact layers and a second layer at high densities. Is also clear that the surface roughness do not affect drastically the layering, but make small changes in the occupancy in each layer. Analyzing only the contact layer is clear that, for all combinations of densities and temperatures, the shape of this peak in the $\rho(z)$ curve are distinct for each wall: in flat surfaces the adsorption peak are higher and thinner, while for the structured surfaces they are lower and thicker.

Is remarkable the layering observed at $T = 0.10$ and $\rho_0 = 0.100$. The fluid is organized in well defined planes along all the simulation box. This specific layering reflects in a anomalous adsorption behavior. In the figure 3(a) we show the adsorption isotherm at $T = 0.10$ as function of the bulk density . As we can see, the density $\rho = 0.100$ corresponds to a maxima in the adsorption. From the 2D phase diagram obtained in our previous study,³¹ we know

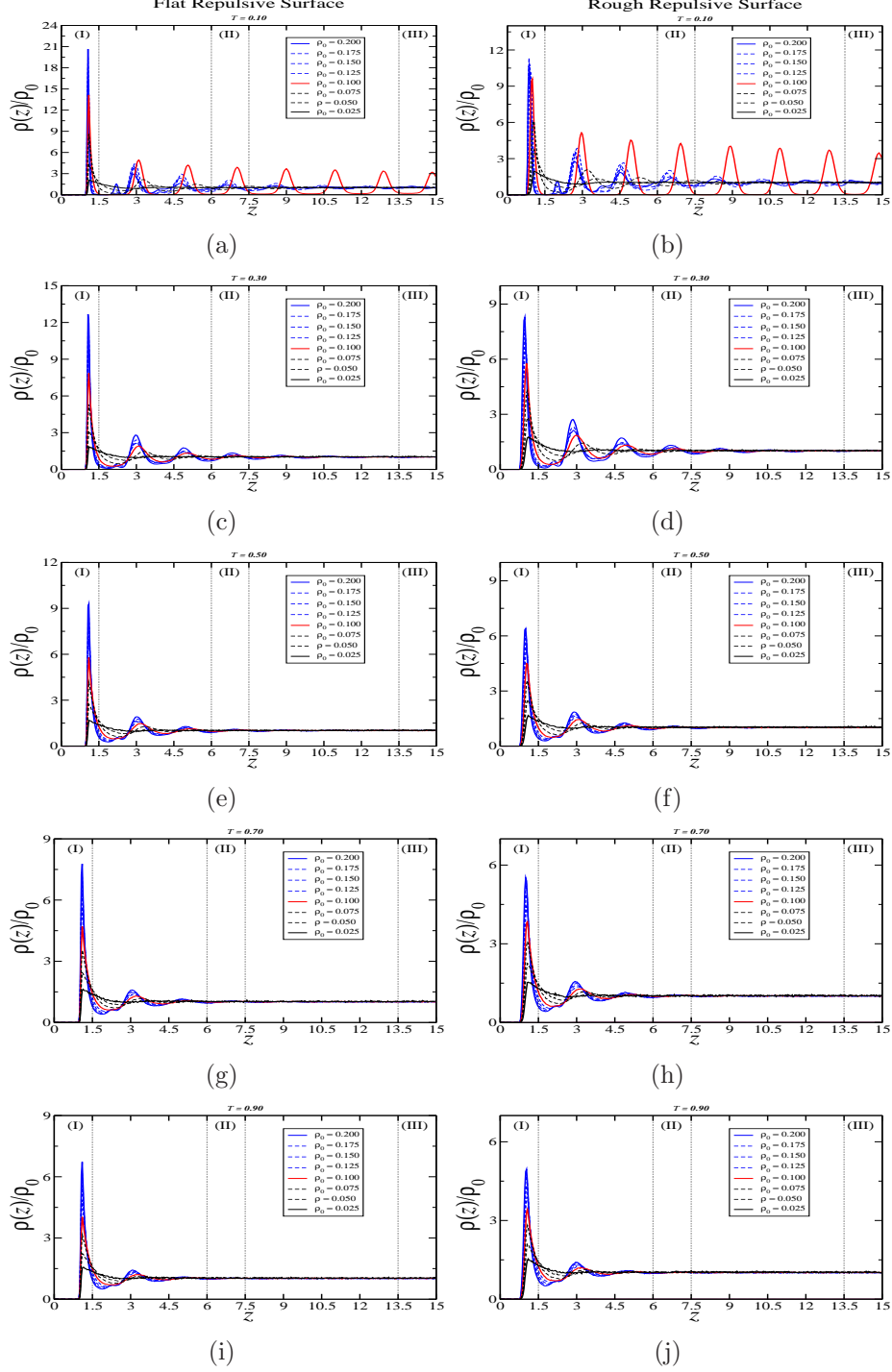


Figure 2: Ramp-like colloids density profile along the z -direction near repulsive walls.

that this point is located in the solid hexagonal phase. Despite the fact that going from 2D to 3D or slab systems can change the phase diagram,^{62–65} each layer at this density is in a hexagonal lattice. Here is clear how the surface structure can affect the fluid layers

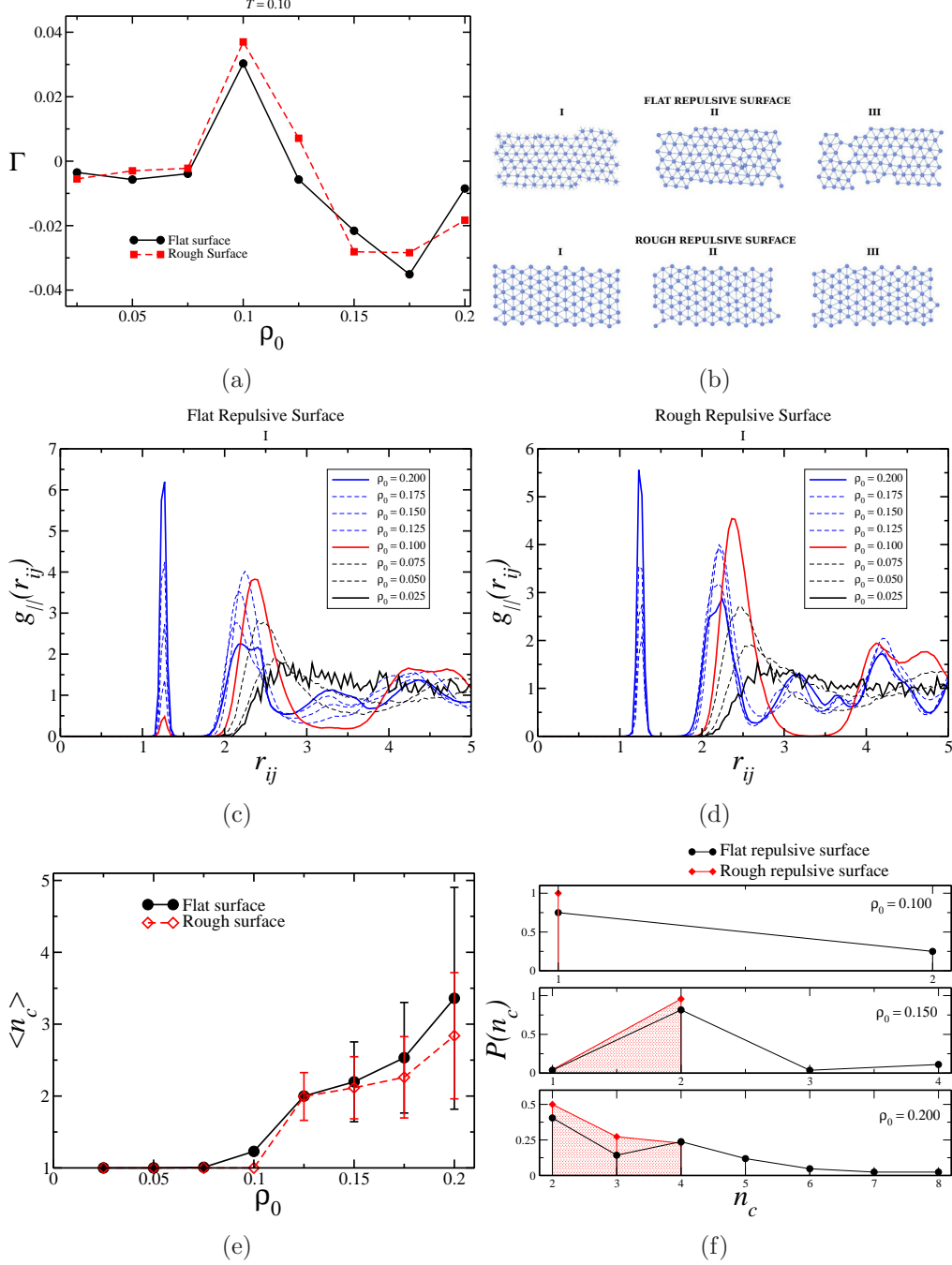


Figure 3: (a) Ramp colloids adsorption isotherm for $T = 0.10$. (b) Layers (I), (II) and (III) structure at the density $\rho_0 = 0.100$ for flat and rough surfaces. LRDF of the contact layer (I) for all densities in (c) flat and (d) rough surfaces. (e) Mean number of particles in one cluster in the contact layer as function of bulk density and (f) probability of find a cluster with size n_c at distinct values of bulk densities.

structure. In the flat surface even the contact layer do not a perfect hexagonal structure, as we show in the upper panel of the figure 3(b). As we move away from the wall more

vacancies and defects can be seen. On the other hand, rough surfaces induces a well defined layering without defects in the hexagonal lattice, as we can see in the bottom panel of the figure 3(b).

We can see the defects by looking at the LRDF of the contact layer (I), shown in figure 3(c) for flat walls and in figure 3(d) for rough walls. As we can see, the overall behavior is similar: at low bulk densities the LRDF indicates no ordering, as in a gas-like phase. As ρ_0 increases, the peak in the LRDF near the second length scale, at $r_2 \approx 2.2$, grows and reach a maximum. At this point, the peak in the LRDF correspondent to the first length scale, at $r_1 \approx 1.2$, appears. However, for flat surfaces, we can see occupancy in the first length scale at $\rho_0 = 0.100$ while the rough surfaces has the higher occupancy in the second length scale and no particles at the first length scale. The occupancy in the first length scale indicates particles aggregation. This is corroborated by the analysis of the mean number of particle in one aggregate cluster at the contact layer (I), shown in the figure 3(e). For flat surfaces and $\rho_0 = 0.100$ the mean cluster size is bigger than 1.0 - indicating the formation of aggregates, while for rough surfaces at $\rho_0 = 0.1$ no cluster were formed - the probability $P(n_c)$ shown in the upper panel of the figure 3(f) also shows this. Increasing the density, the cluster size increases, and the occupancy in the first length scale increases as well.

Increasing T in the 2D system³¹ melts the solid hexagonal phase. Here we observe the same. However, at the intermediate temperatures $T = 0.30$ and $T = 0.50$, the adsorption isotherms show an interesting behavior that can be related to the changes in the occupancy in each length scales. As we shown in figure 4(a), for $T = 0.30$ both surfaces have the anomalous behavior in the adsorption curve, that can be related to the competition between the scales shown in figures 4(b) and (c). For the isotherms at $T = 0.50$ the anomaly remains for the rough surface, but it practically vanishes for the flat surface, as we can see in the figure 4(a). This distinct behavior is also related with the LRDF of the contact layer, shown in figures 4(d) and (e). For the flat surfaces the first length scale is occupied even at low densities, since the thermal energy is high enough to overcome the ramp entalpic contribution

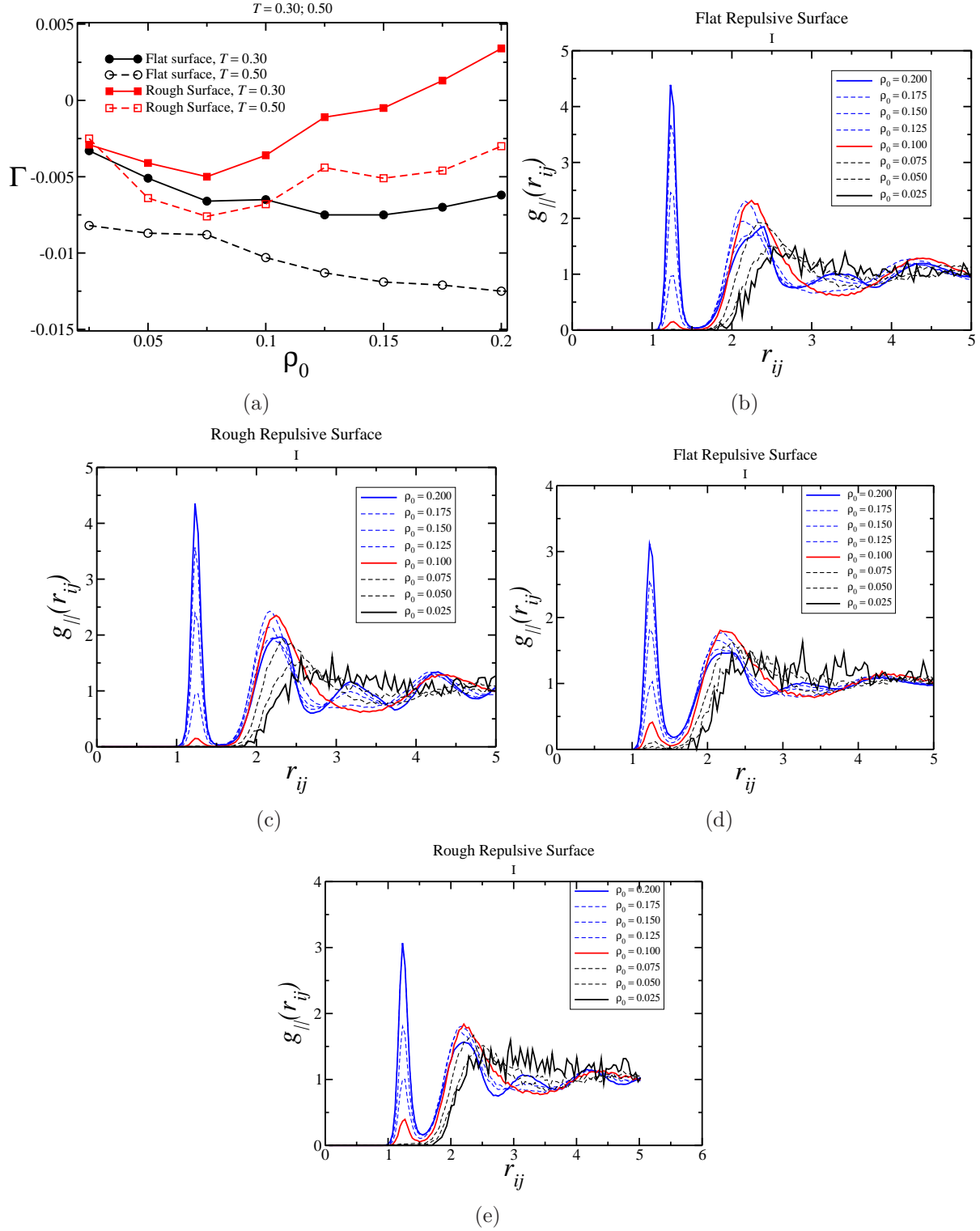


Figure 4: Adsorption isotherms for $T = 0.30$ and $T = 0.50$ (a) and the LRDF for $T = 0.30$ and flat (b) or rough (c) adsorption surfaces and for $T = 0.50$ and flat (d) and or (e) adsorption surfaces

for the total energy. On the other hand, for the rough adsorption surface there is the extra penalty due the friction with the surface beads. As consequence, the competition between the scales and the anomaly is observed for the rough case. So, heating up the system the entropic contribution for the free energy overcome the penalties from the ramp and from the friction, ending the competition, as we show in the figure 5(b) and (c), and the adsorption anomaly, figure 5(a), for $T = 0.90$.

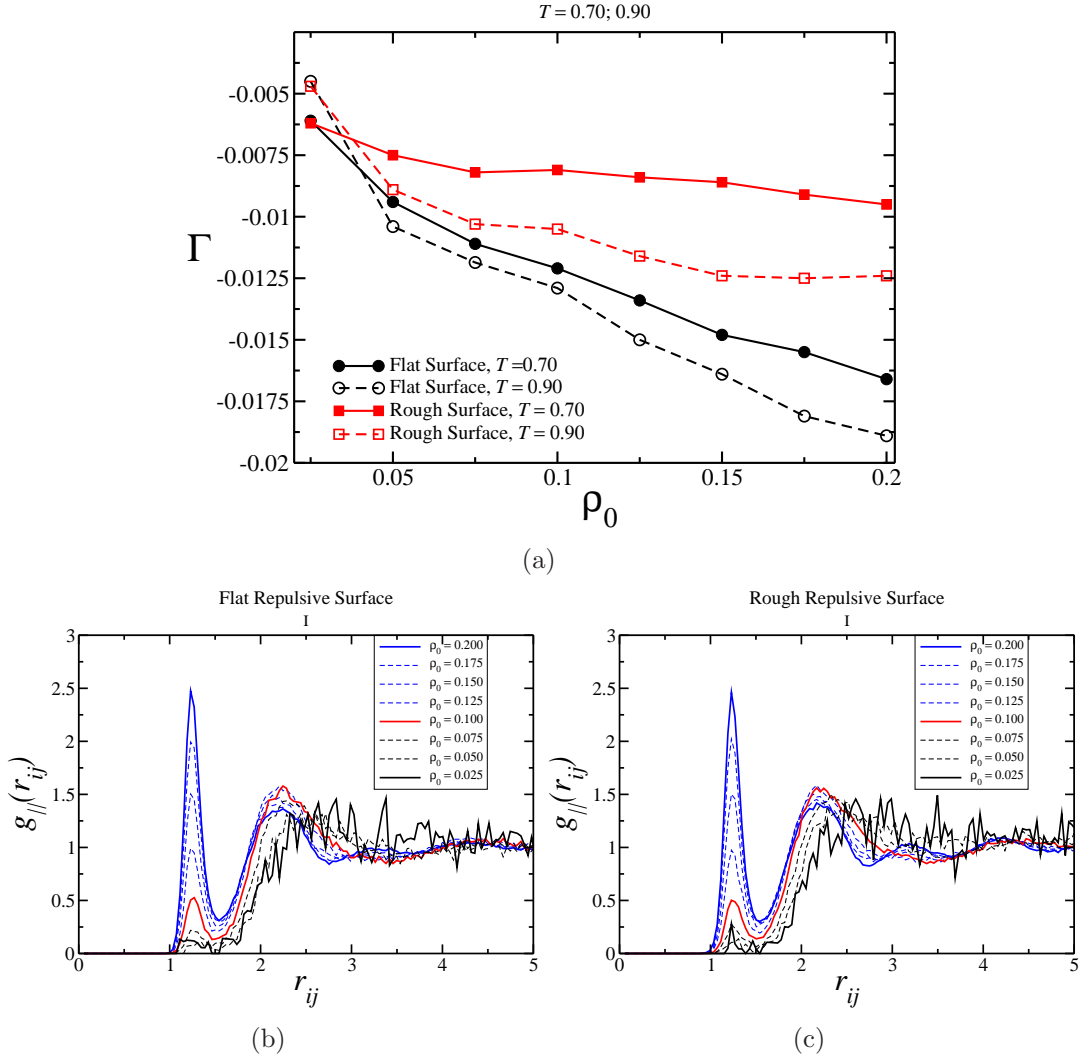


Figure 5: Adsorption isotherms for $T = 0.70$ and $T = 0.00$ (a) and the LRDF for $T = 0.70$ and flat (c) or rough (d) adsorption surfaces.

The competition between the scales observed in the LRDF can be related to the existence of water-like anomalies.⁵⁰ The diffusion anomaly is characterized by the increase in the self-

diffusion constant D as the pressure or density increases. When confined or near surfaces, this anomalous behavior is affected by the surface.⁶⁶⁻⁶⁹ To see how the colloids diffuse at the interface or in the bulk we have evaluated the lateral mean square displacement (LMSD) for distinct layer. With this, we obtain the lateral diffusion constant D_l for each layer, with l ranging from 1, the contact layer, to 15, the layer exactly at the simulation box center where the density was fixed in ρ_0 . Here we show in the figure 6 the contact diffusion D_1 divided by the bulk diffusion D_{15} for all the temperatures. Interesting, for all cases the contact layer diffuses faster at the interface when the colloidal density is small. This is counter-intuitive, once we should expect a smaller diffusion due the friction with the wall. However, core-softened fluids can show a anomalous increase in D near solvophobic surfaces, as we have show previously.^{55,70} As ρ_0 increases, we can see that the isotherms have distinct behaviors. At high T , were no adsorption anomaly was observed, the diffusion decreases with the density. However, for the cases where the system has adsorption anomaly, we observe a diffusion anomaly. The ratio D_1/D_{15} decay with ρ_0 , indicating that the contact layer is diffuse slower than the bulk layers up to a threshold, where the curve has a minimum and increases as ρ_0 increases - similar to the water-like diffusion anomaly. This minima in the diffusion corresponds to the maxima observed for the adsorption, indicating that these quantities are related. This allow us to correlate the adsorption not only to the structure of the adsorbed colloids, but to their dynamic as well.

Conclusions

In this paper we have explored the behavior of SALR particles near solid surfaces. Two species of surfaces were simulated: a flat, smooth surface and a rough, structured one. By controlling the bulk density, we were able to see how the colloids adsorb at the surface at distinct temperatures. As usual for this system, we observe a layering as the density increases at low temperatures. Curiously, the system has more layers at the intermediary simulated

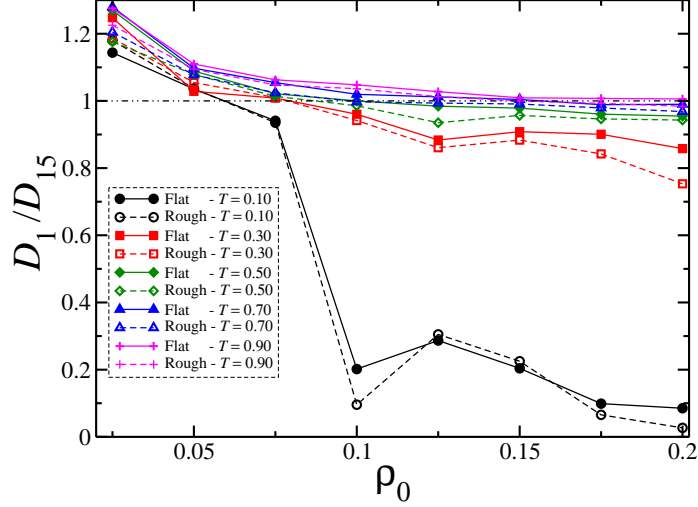


Figure 6: First layer diffusion divided by the central layer (bulk-like) diffusion for distinct bulk densities.

density than at the higher density. This was related with the observation of a triangular lattice in the contact layer. This structural conformation was observed for all layers at $T = 0.10$ and $\rho_0 = 0.100$ - with defects and vacancies in the structure of the layers in the case of flat walls.

This well defined layering at $T = 0.10$ and $\rho_0 = 0.100$ leads to a maxima in the NP adsorption. After that, the colloids start to aggregate. SALR interactions are characterized by the existence of two length scales, the short range attraction and the long range repulsion. This clustering is related to the occupancy in the first length scale - what was not observed prior to the adsorption maxima. Essentially, as ρ_0 increases the packing allow the colloids to overcome the energetic penalty from the long range repulsion. With this, they became closer and start to aggregate. Similarly, the temperatures $T = 0.30$ and $T = 0.50$ have changed in the adsorption curve when the particles starts to occupy the first characteristic distance. However, when T increases, the gain in kinetic energy allow the colloids to overcome the repulsive barrier even at low densities. With this, the first length scale is occupied even at low densities and no maxima is observed in the adsorption.

To check how it is related to the dynamical properties, we evaluated the layer's diffusion and compare the diffusion of the contact layer and the central (bulk-like) layer. We could see

that the maxima in the adsorption corresponds to a minima in the diffusion - this diffusion minima as function of density is similar to the waterlike diffusion anomaly, which is related to competition between the length scales observed in the water molecule interaction.

With this, we could connect adsorption, clustering and diffusion with the competition between the length scales of SALR. In fact, the correlation between maximum in the adsorption and clustering agrees with the recent work by Bildanau and co-workers for 2D systems,⁴⁷ and our results provide information regarding the connection with the diffusion behavior at the interface and the competition between the scales.

Acknowledgement

Without public funding this research would be impossible. MSM thanks the Brazilian Agencies Conselho Nacional de Desenvolvimento Científico e Tecnológico (CNPq) for the PhD Scholarship and Coordenação de Aperfeiçoamento de Pessoal de Nível Superior (CAPES) for the support to the collaborative period in the Instituto de Química Física Rocasolano. JRB acknowledge the Brazilian agencies CNPq and Fundação de Apoio a Pesquisa do Rio Grande do Sul (FAPERGS) for financial support. JRB is greatly indebted to Alexandre Diehl for illuminating discussions. All simulations were performed in the SATOLEP Cluster of the Group of Theory and Simulation in Complex Systems from UFPel.

References

- (1) Dąbrowski, A. Adsorption — from theory to practice. *Advances in Colloid and Interface Science* **2001**, *93*, 135–224.
- (2) *Introduction to Applied Colloid and Surface Chemistry*; John Wiley and Sons, Ltd, 2016; Chapter 7, pp 161–184.
- (3) Bayliss, W. M. The Properties of Colloidal Systems.-II. On Adsorption as Preliminary

- to Chemical Reaction. *Proceedings of the Royal Society of London. Series B, Containing Papers of a Biological Character* **1911**, 84, 81–98.
- (4) Vold, R. D.; Sivaramakrishnan, N. H. The Origin of the Maximum in the Adsorption Isotherms of Association Colloids. *The Journal of Physical Chemistry* **1958**, 62, 984–989.
 - (5) Robens, E.; Jayaweera, S. A. A. Early History of Adsorption Measurements. *Adsorption Science & Technology* **2014**, 32, 425–442.
 - (6) Tareq, R.; Akter, N.; Azam, M. S. In *Biochar from Biomass and Waste*; Ok, Y. S., Tsang, D. C., Bolan, N., Novak, J., Eds.; Elsevier, 2019; pp 169 – 209.
 - (7) Tang, F. *Structures and Dynamics of Interfacial Water: Input from Theoretical Vibrational Sum-frequency Spectroscopy*; Springer Theses; Springer Singapore, 2019.
 - (8) Ciach, A.; Pękalski, J.; Gózdź, W. T. Origin of similarity of phase diagrams in amphiphilic and colloidal systems with competing interactions. *Soft Matter* **2013**, 9, 6301–6308.
 - (9) Campbell, A. I.; Anderson, V. J.; van Duijneveldt, J. S.; Bartlett, P. Dynamical Arrest in Attractive Colloids: The Effect of Long-Range Repulsion. *Phys. Rev. Lett.* **2005**, 94, 208301.
 - (10) Adamczyk, Z.; Weroński, P.; Musiał, E. Colloid Particle Adsorption at Random Site (Heterogeneous) Surfaces. *Journal of Colloid and Interface Science* **2002**, 248, 67 – 75.
 - (11) Adamczyk, Z. Modeling adsorption of colloids and proteins. *Current Opinion in Colloid & Interface Science* **2012**, 17, 173 – 186.
 - (12) Wasilewska, M.; Adamczyk, Z. Fibrinogen Adsorption on Mica Studied by AFM and in Situ Streaming Potential Measurements. *Langmuir* **2011**, 27, 686–696, PMID: 21155546.

- (13) Rahmani, A. M.; Wang, A.; Manoharan, V. N.; Colosqui, C. E. Colloidal particle adsorption at liquid interfaces: capillary driven dynamics and thermally activated kinetics. *Soft Matter* **2016**, *12*, 6365–6372.
- (14) Imperio, A.; Reatto, L. Microphase morphology in two-dimensional fluids under lateral confinement. *Phys. Rev. E* **2007**, *76*, 040402.
- (15) Rabe, M.; Verdes, D.; Seeger, S. Understanding protein adsorption phenomena at solid surfaces. *Advances in Colloid and Interface Science* **2011**, *162*, 87 – 106.
- (16) Stradner, A.; Schurtenberger, P. Potential and limits of a colloid approach to protein solutions. *Soft Matter* **2020**, *16*, 307–323.
- (17) Santos, A. P.; Pekalski, J.; Panagiotopoulos, A. Z. Thermodynamic signatures and cluster properties of self-assembly in systems with competing interactions. *Soft Matter* **2017**, *13*, 8055–8063.
- (18) Verwey, E.; Overbeek, J.; van Nes, K. *Theory of the Stability of Lyophobic Colloids: The Interaction of Sol Particles Having an Electric Double Layer*; Elsevier Publishing Company, 1948.
- (19) Asakura, S.; Oosawa, F. On Interaction between Two Bodies Immersed in a Solution of Macromolecules. *The Journal of Chemical Physics* **1954**, *22*, 1255–1256.
- (20) Asakura, S.; Oosawa, F. Interaction between particles suspended in solutions of macromolecules. *Journal of Polymer Science* **1958**, *33*, 183–192.
- (21) Royall, C. P. Hunting mermaids in real space: known knowns, known unknowns and unknown unknowns. *Soft Matter* **2018**, *14*, 4020–4028.
- (22) Shukla, A.; Mylonas, E.; Di Cola, E.; Finet, S.; Timmins, P.; Narayanan, T.; Svergun, D. I. Absence of equilibrium cluster phase in concentrated lysozyme solutions. *Proceedings of the National Academy of Sciences* **2008**, *105*, 5075–5080.

- (23) Somerville, W. R. C.; Law, A. D.; Rey, M.; Vogel, N.; Archer, A. J.; Buzza, D. M. A. Pattern formation in two-dimensional hard-core/soft-shell systems with variable soft shell profiles. *Soft Matter* **2020**, *16*, 3564–3573.
- (24) Cardoso, D. S.; Hernandez, V. F.; Nogueira, T.; Bordin, J. R. Structural behavior of a two length scale core-softened fluid in two dimensions. *Physica A: Statistical Mechanics and its Applications* **2021**, *566*, 125628.
- (25) Pekalski, J.; Ciach, A.; Almarza, N. G. Periodic ordering of clusters and stripes in a two-dimensional lattice model. I. Ground state, mean-field phase diagram and structure of the disordered phases. *The Journal of Chemical Physics* **2014**, *140*, 114701.
- (26) Ong, G. K.; Williams, T. E.; Singh, A.; Schaible, E.; Helms, B. A.; Milliron, D. J. Ordering in Polymer Micelle-Directed Assemblies of Colloidal Nanocrystals. *Nano Letters* **2015**, *15*, 8240–8244.
- (27) Montes-Campos, H.; Otero-Mato, J. M.; Mendez-Morales, T.; Cabeza, O.; Gallego, L. J.; Ciach, A.; Varela, L. M. Two-dimensional pattern formation in ionic liquids confined between graphene walls. *Phys. Chem. Chem. Phys.* **2017**, *19*, –.
- (28) Quesada-Perez, M.; Moncho-Jorda, A.; Martinez-Lopez, F.; Hidalgo-Álvarez, R. Probing interaction forces in colloidal monolayers: Inversion of structural data. *Journal of Chemical Physics* **2001**, *115*, 10897.
- (29) Contreras-Aburto, C.; and R.C. Priego, J. M. Structure and effective interactions in parallel monolayers of charged spherical colloids. *Journal of Chemical Physics* **2010**, *132*, 174111.
- (30) Haddadi, S.; Skepö, M.; Jannasch, P.; Manner, S.; Forsman, J. Building polymer-like clusters from colloidal particles with isotropic interactions, in aqueous solution. *Journal of Colloid and Interface Science* **2020**, *581*, 669–681.

- (31) S. Marques, M.; P. O. Nogueira, T.; F. Dillenburg, R.; C. Barbosa, M.; Bordin, J. R. Waterlike anomalies in hard core–soft shell nanoparticles using an effective potential approach: Pinned vs adsorbed polymers. *Journal of Applied Physics* **2020**, *127*, 054701.
- (32) Lafitte, T.; Kumar, S. K.; Panagiotopoulos, A. Z. Self-assembly of polymer-grafted nanoparticles in thin films. *Soft Matter* **2014**, *10*, 786–794.
- (33) Curk, T.; Martinez-Veracoechea, F. J.; Frenkel, D.; Dobnikar, J. Nanoparticle Organization in Sandwiched Polymer Brushes. *Nano Letters* **2014**, *14*, 2617–2622.
- (34) Nie, G.; Li, G.; Wang, L.; Zhang, X. Nanocomposites of polymer brush and inorganic nanoparticles: preparation, characterization and application. *Polym. Chem.* **2016**, *7*, 753–769.
- (35) Wang, Z.; Zheng, Z.; Liu, J.; Wu, Y.; Zhang, L. Tuning the Mechanical Properties of Polymer Nanocomposites Filled with Grafted Nanoparticles by Varying the Grafted Chain Length and Flexibility. *Polymers* **2016**, *8*, 270.
- (36) Bos, I.; van der Scheer, P.; Ellenbroek, W. G.; Sprakel, J. Two-dimensional crystals of star polymers: a tale of tails. *Soft Matter* **2019**, *15*, 615–622.
- (37) Jagla, E. A. Phase behavior of a system of particles with core collapse. *Phys. Rev. E* **1998**, *58*, 1478.
- (38) Saija, F.; Prestipino, S.; Malescio, G. Anomalous phase behavior of a soft-repulsive potential with a strictly monotonic force. *Physical Review E* **2009**, *80*, 031502.
- (39) Malescio, G.; Saija, F. A Criterion for Anomalous Melting in Systems with Isotropic Interactions. *The Journal of Physical Chemistry B* **2011**, *115*, 14091–14098.
- (40) Prestipino, S.; Saija, F.; Malescio, G. Anomalous phase behavior in a model fluid with only one type of local structure. *Journal of Chemical Physics* **2010**, *133*, 144504.

- (41) Prestipino, S.; Saija, F.; Giaquinta, P. V. Hexatic phase and water-like anomalies in a two-dimensional fluid of particles with a weakly softened core. *Journal of Chemical Physics* **2012**, *137*, 104503.
- (42) Coslovich, D.; Ikeda, A. Cluster and reentrant anomalies of nearly Gaussian core particles. *Soft Matter* **2013**, *9*, 6786.
- (43) Almarza, N. G.; Pekalski, J.; Ciach, A. Effects of confinement on pattern formation in two dimensional systems with competing interactions. *Soft Matter* **2016**, *12*, 7551–7563.
- (44) Litniewski, M.; Ciach, A. Effect of aggregation on adsorption phenomena. *The Journal of Chemical Physics* **2019**, *150*, 234702.
- (45) Pekalski, J.; Bildanau, E.; Ciach, A. Self-assembly of spiral patterns in confined systems with competing interactions. *Soft Matter* **2019**, *15*, 7715–7721.
- (46) Pekalski, J.; Rządkowski, W.; Panagiotopoulos, A. Z. Shear-induced ordering in systems with competing interactions: A machine learning study. *The Journal of Chemical Physics* **2020**, *152*, 204905.
- (47) Bildanau, E.; Pekalski, J.; Vikhrenko, V.; Ciach, A. Adsorption anomalies in a two-dimensional model of cluster-forming systems. *Phys. Rev. E* **2020**, *101*, 012801.
- (48) Salcedo, E.; de Oliveira, A. B.; Barraz, N. M.; Chakravarty, C.; Barbosa, M. C. Core-softened fluids, water-like anomalies, and the liquid-liquid critical points. *The Journal of Chemical Physics* **2011**, *135*, 044517.
- (49) Fomin, Y. D.; Tsiok, E. N.; Ryzhov, V. N. Inversion of sequence of diffusion and density anomalies in core-softened systems. *The Journal of Chemical Physics* **2011**, *135*, 234502.
- (50) Barraz, N. M.; Salcedo, E.; Barbosa, M. C. Thermodynamic, dynamic, and structural anomalies for shoulderlike potentials. *The Journal of Chemical Physics* **2009**, *131*, 094504.

- (51) da Silva, J. N.; Salcedo, E.; de Oliveira, A. B.; Barbosa, M. C. Effects of the attractive interactions in the thermodynamic, dynamic, and structural anomalies of a two length scale potential. *The Journal of Chemical Physics* **2010**, *133*, 244506.
- (52) Limbach, H.-J.; Arnold, A.; Mann, B. A.; Holm, C. ESPResSo - An Extensible Simulation Package for Research on Soft Matter Systems. *Comput. Phys. Commun.* **2006**, *174*, 704–727.
- (53) Arnold, A.; Lenz, O.; Kesselheim, S.; Weeber, R.; Fahrenberger, F.; Roehm, D.; Kosovan, P.; Holm, C. In *Meshfree Methods for Partial Differential Equations VI*; Griebel, M., Schweitzer, M. A., Eds.; Lecture Notes in Computational Science and Engineering; Springer Berlin Heidelberg, 2013; Vol. 89; pp 1–23.
- (54) Bordin, J. R.; Diehl, A.; Barbosa, M. C.; Levin, Y. Ion fluxes through nanopores and transmembrane channels. *Phys. Rev. E* **2012**, *85*, 031914.
- (55) Bordin, J. R.; Diehl, A.; Barbosa, M. C. Relation Between Flow Enhancement Factor and Structure for Core-Softened Fluids Inside Nanotubes. *The Journal of Physical Chemistry B* **2013**, *117*, 7047–7056, PMID: 23692639.
- (56) Bordin, J. R.; Andrade, J. S.; Diehl, A.; Barbosa, M. C. Enhanced flow of core-softened fluids through narrow nanotubes. *The Journal of Chemical Physics* **2014**, *140*, 194504.
- (57) Allen, M.; Tildesley, D. *Computer Simulation of Liquids: Second Edition*; OUP Oxford, 2017.
- (58) Krott, L. B.; Bordin, J. R.; Barbosa, M. C. New Structural Anomaly Induced by Nanoconfinement. *The Journal of Physical Chemistry B* **2015**, *119*, 291–300, PMID: 25494049.
- (59) Toledano, J. C. F.; Sciortino, F.; Zaccarelli, E. Colloidal systems with competing in-

- teractions: from an arrested repulsive cluster phase to a gel. *Soft Matter* **2009**, *5*, 2390–2398.
- (60) Rafael Bordin, J. Distinct self-assembly aggregation patterns of nanorods with decorated ends: A simple model study. *Fluid Phase Equilibria* **2019**, *499*, 112251.
- (61) Bordin, J. R. Distinct aggregation patterns and fluid porous phase in a 2D model for colloids with competitive interactions. *Physica A: Statistical Mechanics and its Applications* **2018**, *495*, 215 – 224.
- (62) Dudalov, D. E.; Fomin, Y. D.; Tsiok, E. N.; Ryzhov, V. N. How dimensionality changes the anomalous behavior and melting scenario of a core-softened potential system? *Soft Matter* **2014**, *10*, 4966.
- (63) Fomin, Y. D.; Ryzhov, V. N.; Tsiok, E. N. Interplay between freezing and density anomaly in a confined core-softened fluid. *Molecular Physics* **2020**, *118*, e1718792.
- (64) Bordin, J. R.; Barbosa, M. C. Waterlike anomalies in a two-dimensional core-softened potential. *Phys. Rev. E* **2018**, *97*, 022604.
- (65) Krott, L.; Bordin, J. R. Distinct dynamical and structural properties of a core-softened fluid when confined between fluctuating and fixed walls. *Journal of Chemical Physics* **2013**, *139*, 154502.
- (66) Köhler, M. H.; Bordin, J. R.; de Matos, C. F.; Barbosa, M. C. Water in nanotubes: The surface effect. *Chemical Engineering Science* **2019**, *203*, 54 – 67.
- (67) Köhler, M. H.; Bordin, J. R.; da Silva, L. B.; Barbosa, M. C. Structure and dynamics of water inside hydrophobic and hydrophilic nanotubes. *Physica A: Statistical Mechanics and its Applications* **2018**, *490*, 331 – 337.
- (68) Bordin, J. R.; Barbosa, M. C. Flow and structure of fluids in functionalized nanopores. *Physica A: Statistical Mechanics and its Applications* **2017**, *467*, 137 – 147.

- (69) Nogueira, T. P. O.; Frota, H. O.; Piazza, F.; Bordin, J. R. Tracer diffusion in crowded solutions of sticky polymers. *Phys. Rev. E* **2020**, *102*, 032618.
- (70) Bordin, J. R.; de Oliveira, A. B.; Diehl, A.; Barbosa, M. C. Diffusion enhancement in core-softened fluid confined in nanotubes. *The Journal of Chemical Physics* **2012**, *137*, 084504.